6384 *Inorg. Chem.* **2010**, *49*, 6384–6386
DOI: 10.1021/ic1007928

Inorganic Chemistry
Communication

Understanding Eu^{3+} Emission by Using ^{15}N Vibronic Shifts

Wenyu Li and Peter A. Tanner*

Department of Biology and Chemistry, City University of Hong Kong, Tat Chee Avenue, Kowloon, Hong Kong SAR, People's Republic of China

Received April 23, 2010

Hexanitritolanthanates provide a unique opportunity to investigate the energy-level structures and crystal field of the lanthanide ion (Ln^{3+}) in T_h site symmetry, with 12-coordination to oxygen. However, the electronic spectra are mainly vibronic and particularly extensive and complex. Advantage may be taken of the high energy of NO_2^- vibrations, using ^{15}N substitution, in assigning the electronic emission spectra. These features form a fingerprint in less-congested spectral regions. The technique is demonstrated for the case of Ln = Eu, from the study of the $^5D_0$ emission spectra.

The electronic spectra of Eu^{3+} doped into high-symmetry elpasolite host crystals have been extensively studied.[1−4] The results enabled the deduction of the $4f^6$ electronic energy levels of Eu^{3+} at an octahedral site symmetry and the crystal-field parametrization of the energy-level scheme. Richardson and co-workers also pioneered calculation of the vibronic intensities for this system, where the $4f^N-4f^N$ electronic transitions are electric-dipole-forbidden but the one-phonon vibronic sideband is enabled by this mechanism. Most studies of Eu^{3+} spectra have been carried out with noncentrosymmetric crystals so that the vibronic sidebands are buried within much stronger forced-dipole electronic transitions. We therefore searched for other centrosymmetric systems where a comparison could be made with the spectra of EuF_6^{3-} and $EuCl_6^{3-}$. The versatile nitrite ligand is a suitable candidate because it forms chelating bidentate coordination with lanthanide (Ln^{3+}) ions,[5] unlike the mainly monodentate nitrito and *N*-ligated nitro complexes with transition metals.[6−8] The Ln^{3+} ion occupies a T_h site in the $Cs_2NaLn(NO_2)_6$ systems[9] and is surrounded by six NO_2^- ions, as shown in Figure 1. Some previous investigations[10,11] have shown that the electronic spectra are very complex because they are almost entirely vibronic in nature, so that comprehensive investigations have not yet been performed. It is the purpose of the present study to show that the characteristic ligand vibronic fingerprint may considerably aid interpretation of the electronic spectra. This requires a clear understanding of not only the vibrational properties of the nitrite anion but also the effects of ^{15}N substitution. Isotopic shifts of bands in the electronic emission spectra can then be employed to delineate an accurate energy-level scheme for Eu^{3+} in this novel site symmetry.

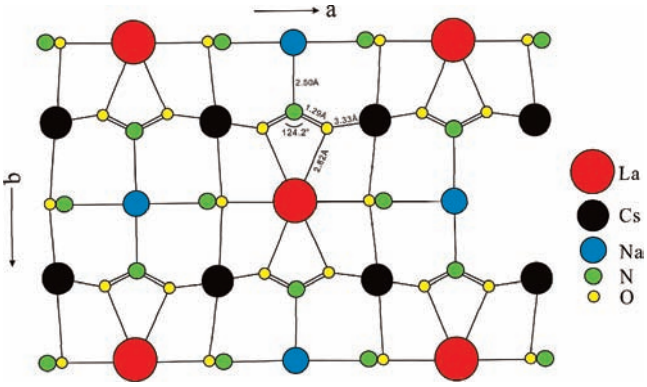

Figure 1. Crystal structure of $Cs_2NaLa(NO_2)_6$ viewed down the *c* axis (adapted from ref 5).

The syntheses of $Cs_2NaEu(NO_2)_6$ crystals with natural isotopic abundance (99.6% ^{14}N: denoted as ^{14}N hereafter) and 99% ^{15}N labeling (denoted as ^{15}N hereafter) were made from $Cs_2NaEuCl_6$ and $NaNO_2$ at neutral pH, as described in the Supporting Information. In the T_h site symmetry of the $Ln(NO_2)_6^{3-}$ moiety, three N−O stretching vibrations (α_g, ε_g, and τ_g) are Raman-active, whereas the symmetric and antisymmetric N−O stretching modes (both τ_u) are IR-active. These stretching modes are the highest-energy fundamental vibrations, with the NO_2^- scissor modes (α_g and ε_g, Raman-active; τ_u, IR-active) being the next-highest-energy vibrations. Figure 2a displays the Raman spectra of $Cs_2NaEu(NO_2)_6$, with ^{14}N and ^{15}N labeling. In the ^{14}N spectrum,

*To whom correspondence should be addressed. E-mail: bhtan@cityu.edu.hk.

(1) Serra, O. A.; Thompson, L. C. *Inorg. Chem.* **1976**, *15*, 504.
(2) Morley, J. P.; Faulkner, T. R.; Richardson, F. S. *J. Chem. Phys.* **1982**, *77*, 1710.
(3) Tanner, P. A.; Liu, Y.-L. *J. Alloys Compd.* **1994**, *204*, 93.
(4) Tanner, P. A.; Liu, Y.-L.; Edelstein, N.; Murdoch, K.; Khaidukov, N. M. *J. Phys.: Condens. Matter* **1997**, *9*, 7817.
(5) Barnes, J. C.; Al-Rasoul, K.; Harkins, P. *J. Chem. Soc. Pak.* **1980**, *2*, 9.
(6) Caulton, K. G.; Fenske, R. F. *Inorg. Chem.* **1967**, *6*, 562.
(7) Krause, R. A.; Wickenden, A. E.; Ruggles, C. R. *Inorg. Chem.* **1966**, *5*, 936.
(8) Fee, W. W.; Garner, C. S.; Harrowfield, J. N. M. *Inorg. Chem.* **1967**, *6*, 87.
(9) Roser, M. R.; Corruccini, L. R. *Phys. Rev. B* **1990**, *41*, 2359.
(10) Nissen-Sobocińska, B.; Łukowiak, E.; Strek, W.; Luxbacher, T.; Fritzer, H. P.; Xie, R.-Q.; Flint, C. D. *SPIE* **1997**, *3176*, 130.
(11) Bünzli, J.-C.; Petaud, G. S.; Moret, E. *Spectrosc. Lett.* **1999**, *32*, 155.

Published on Web 06/14/2010

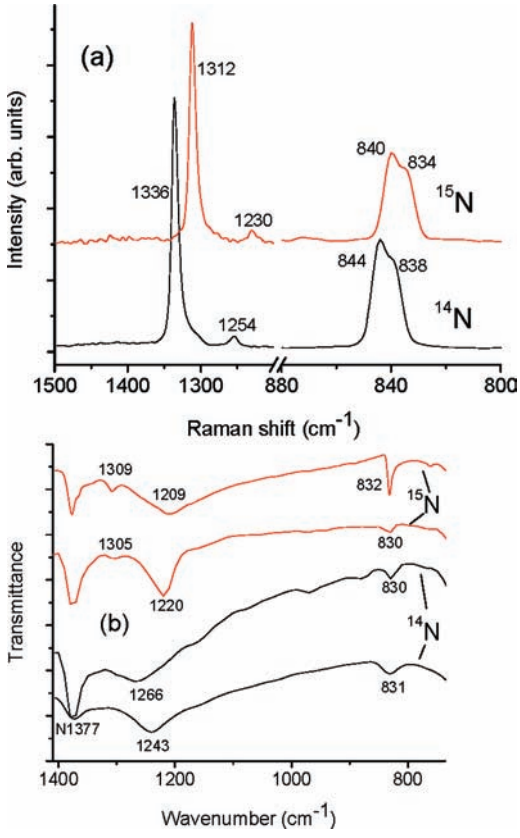

Figure 2. FT-Raman (a) and FT-IR (b) spectra of ^{14}N- and ^{15}N-labeled $Cs_2NaEu(NO_2)_6$ at 300 K.

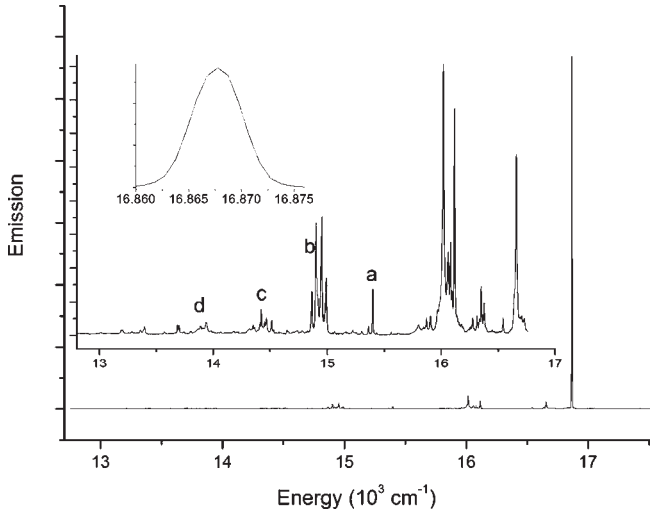

Figure 3. Survey 425 nm excited 15 K emission spectrum of $Cs_2NaEu_{0.01}Y_{0.99}(NO_2)_6$ between 17 500 and 12 500 cm^{-1}. The insets show a scale expansion of the region below 16 760 cm^{-1}, together with the detail of the $^5D_0 \rightarrow {}^7F_1$ zero-phonon line at 16 868 cm^{-1}.

two stretching modes are at 1254 and 1336 cm^{-1}. These bands move ~24 cm^{-1} to lower energy in the ^{15}N spectrum. The α_g and ε_g Raman-active scissor vibrations are assigned at 844 and 838 cm^{-1}, respectively, and these move 4 cm^{-1} to lower energy in the ^{15}N spectrum. It is evident from the FT-IR spectra of two different samples of $Cs_2NaEu(NO_2)_6$ in Figure 2b why previous reports[11,12] have shown disagreement.

(12) Barnes, J. C.; Peacock, R. D. *J. Chem. Soc. A* **1971**, 558.

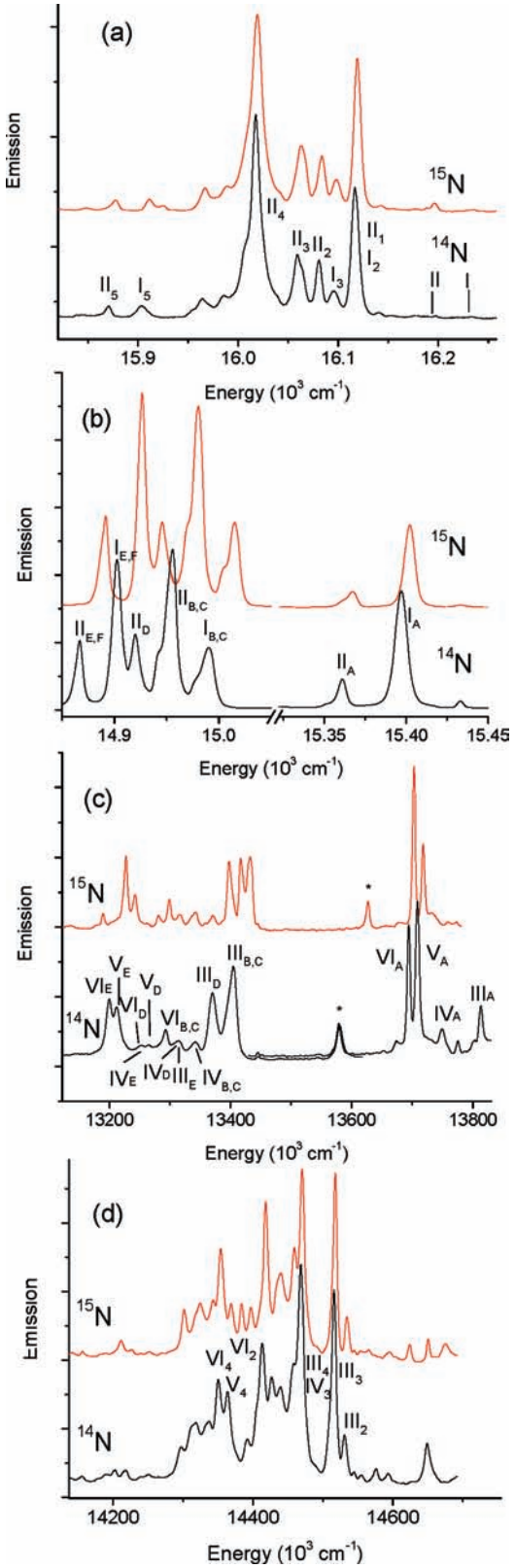

Figure 4. Comparison of 425 nm excited 20 K emission spectra of ^{14}N- and ^{15}N-labeled $Cs_2NaEu(NO_2)_6$: (a) 16 250−15 820 cm^{-1}; (b) 15 450−14 850 cm^{-1} (note the scale break); (c) 13 830−13 120 cm^{-1} (the ^{14}N spectrum below 13 620 cm^{-1} is at 100 K, as shown by the overlap); (d) 14 755−14 136 cm^{-1}. Refer to the text for band identifications.

The Nujol band at 1377 cm^{-1} is marked in the spectra (N), and the major difference relates to the N−O stretching mode,

which moves from 1243 to 1266 cm^{-1} in the spectra of two ^{14}N samples. The shift is not due to the NO_3^- impurity (the presence of which is most readily monitored by the intense Raman band at ~1050 cm^{-1}) or the presence of water but is attributed to other unidentified impurities. The lower FT-IR spectrum (and other spectra, not shown) exhibits a sharper structure of the ~1243 cm^{-1} band, which moves ~23 cm^{-1} to lower energy for the ^{15}N sample. The latter spectrum displays another band at 1305 cm^{-1}, which is at higher energy and is hidden in the Nujol peak in the ^{14}N spectrum but is estimated to be at ~1305 + 23 cm^{-1}. The τ_u NO_2 scissor mode is at 831 cm^{-1} at 300 K.

Figure 3 shows the survey electronic emission spectrum of Eu^{3+} doped into $Cs_2NaY(NO_2)_6$ at ~1 atom %, excited by 425 nm radiation, which comprises luminescence from the initial $^5D_1$ and $^5D_0$ multiplets. The strongest feature is the $^5D_0 \rightarrow {}^7F_1$ magnetic-dipole-allowed zero-phonon line at 16 868 cm^{-1}, and this is shown in more detail in the inset. Structures a−d are subsequently described. As mentioned above, pure electronic transitions are electric-dipole-forbidden for Eu^{3+} ions situated at centrosymmetric sites. The lower-energy part of the spectrum is amplified for clarity and is very complex but similar to the emission spectrum of neat $Cs_2NaEu(NO_2)_6$, which is now discussed.

Figure 4a shows the $^5D_0$ (A_g) → $^7F_2$ (E_g, T_g) emission spectra of ^{14}N- and ^{15}N-labeled $Cs_2NaEu(NO_2)_6$. The entire structure is vibronic in nature, and the strongest bands are assigned to bending modes involving Eu^{3+} motion, coupled with low-energy NO_2^- and lattice modes. We do not attempt specific assignments here but note that two electronic origins can be assigned from the vibronic analysis at 16 193, and 16 229 cm^{-1}, in the ^{14}N spectrum, labeled as II and I, respectively. The vibrations based upon these origins are labeled as subscripts 1−5. The origins shift by ~3 cm^{-1} in the ^{15}N spectrum, but the $^{14}N-{}^{15}N$ vibrational energy shifts are small so that the bands are almost superimposed in the figure. There is, therefore, a characteristic separation of 36 cm^{-1} observed between vibrations based upon origins I and II in the ^{14}N spectrum.

Figure 4b shows the region between 15 450 and 14 850 cm^{-1} (regions a and b in Figure 3), and by contrast to Figure 4a, there are marked band shifts between the ^{14}N and ^{15}N spectra. The separations of some spectral features by 36 cm^{-1} enable assignments to be made for structures based upon I and II, as labeled in the diagram. The derived vibrational energies in the ^{14}N case are (A) 835 cm^{-1}, (B,C) 1240, and 1255 cm^{-1}, (D) 1276 cm^{-1}, and (E,F) 1328, and 1335 cm^{-1}. The feature A correlates with the τ_u scissors mode, and the strongest features to lower energy, B and E, correlate with the τ_u symmetric and antisymmetric N−O stretches. The weaker features, C (ε_g) and F (α_g), are associated with Raman-active N−O stretching modes. The assignment of the vibration at 1276 cm^{-1} requires further investigation, but it could correspond to the (unobserved) τ_g mode. Now we can employ this vibronic fingerprint to assign other transitions.

Figure 4c shows the spectral region between 13 830 and 13 120 cm^{-1} (region d in Figure 3). These bands correspond to NO_2^- modes based upon the four $^5D_0 \rightarrow {}^7F_4$ zero-phonon lines, which we label III−VI for convenience. However, the starred band exhibits a very large $^{14}N-{}^{15}N$ shift of ~48 cm^{-1}, and because it is situated at 2652 cm^{-1} to low energy of I, it therefore corresponds to one quantum of the α_g NO_2^- stretch based upon I_E. From the $^{14}N-{}^{15}N$ shifts, other bands can be assigned to the vibrational structure based upon III−VI, despite spectral congestion. The origins are thus inferred to be at (in cm^{-1}) 14 647 (III), 14 586 (IV), 14 544 (V), and 14 530 (VI). This spectral region is very complex, as shown in Figure 4d, and a priori it would be difficult to make band assignments. However, given the information of III−VI, the respective low-energy bending vibration sidebands can now be assigned, as shown in Figure 4d (corresponding to region c in Figure 3), to features with small isotopic shifts. Other structure is superimposed upon these features, and it is noted that the bands due to the electronic zero-phonon lines of $^5D_0 \rightarrow {}^7F_4$ are not expected to be prominent.

In conclusion, the study of hexanitritolanthanates is interesting not only because the bidentate chelating coordination of the NO_2^- group differs from that in the transition-metal NO_2^- complexes but also because the high Ln^{3+} site symmetry permits a detailed comparison and evaluation with the spectra and crystal-field results of lanthanide elpasolite systems. The present study has demonstrated the feasibility of interpretation and assignment of the complex electronic spectra of $Cs_2NaLn(NO_2)_6$ systems.

Acknowledgment. Financial support from the Hong Kong University Grants Council General Research Fund project CityU 102609 is gratefully acknowledged.

Supporting Information Available: Synthesis and experimental details. This material is available free of charge via the Internet at http://pubs.acs.org.